PAPER

The manipulation of an unstarting supersonic flow by plasma actuator

J. Phys. D: Appl. Phys. **45** (2012) 485202 (8pp) doi:10.1088/0022-3727/45/48/485202

The manipulation of an unstarting supersonic flow by plasma actuator

S Im[1], H Do[2] and M A Cappelli[1]

[1] Mechanical Engineering Department, Stanford University, Stanford, CA 94305-3032, USA
[2] Department of Aerospace and Mechanical Engineering, University of Notre Dame, Notre Dame, IN 46556-5637, USA

E-mail: sim3@stanford.edu

Received 4 September 2012, in final form 17 October 2012
Published 6 November 2012
Online at stacks.iop.org/JPhysD/45/485202

Abstract
The manipulation of an unstarting supersonic flow is demonstrated using a dielectric barrier discharge (DBD). Experiments are carried out in a Mach 4.7 model inlet flow. Flow features, such as boundary layers and shockwaves at low freestream static pressure (1 kPa) and temperature (60 K) are visualized with Rayleigh scattering from condensed CO_2 particles. Flow unstart, initiated by mass injection, is studied for three model inlet flow configurations, distinguished by the initial conditions (untripped or tripped, plasma actuated or not) of the boundary layers. Unstart in the presence of thick, tripped boundary layers is characterized by the formation of an oblique unstart shock just upstream of a separating and propagating boundary layer. The presence of plasma actuation of this tripped boundary layer seems to arrest the boundary layer separation and leads to the formation of a quasi-stationary pseudo-shock, delaying unstart. The flow generated with DBD actuation is more characteristic of what is seen when unstart is generated in a model flow in which thin boundary layers grow naturally. Planar laser Rayleigh scattering visualizations suggest that the DBD actuation thins the tripped boundary layer over the exposed electrode region.

(Some figures may appear in colour only in the online journal)

1. Introduction

There have been several studies investigating unstart, a condition that can cause scramjet engine malfunction (Emami *et al* 1995, Wieting 1976, Rodi *et al* 1996, O'Bryne *et al* 2000). It is believed that the thermal choking of the internal supersonic flow that results from the heat release in the combustor is the primary cause of unstart (Mashio *et al* 2001, Kodera *et al* 2003). An abrupt pressure rise followed by heat release in the inlet duct leads to boundary layer growth and separation (Heiser and Pratt 1994, McDaniel and Edwards 2001). This disturbance can propagate upstream and generate blockage ('unstart' of the upstream flow), resulting in a transition to subsonic flow within the inlet. While it is difficult to reproduce combustion-driven unstart for typical flight conditions in ground test facilities, the physics of this unstart process can be studied by partially reproduced flight conditions. For example, Wagner *et al* (2008) studied the formation and dynamics of an unstart shock system in a model inlet (non-combusting) flow within a ground test facility that mimics the flow blockage caused by thermal chocking through the use of a mechanical flap. In a similar model inlet flow that generates blockage by downstream mass injection, Do *et al* (2011a, 2011b) found that the boundary layer growth and separation leading to unstart are strongly coupled to the boundary layer conditions. Apparent from these prior unstart studies is that the control or actuation of boundary layers in a scramjet inlet can provide a potential mechanism of delaying or possibly even preventing unstart, extending engine performance and operating margin.

Prior studies of unstart delay and prevention include the use of isolators (Curran *et al* 1996, Sato *et al* 1997, Wang and Le 2000, Tam *et al* 2008) and boundary layer bleed (Kodera *et al* 2003). In this paper, we present a study aimed at evaluating the effectiveness of a dielectric barrier discharge (DBD), through the actuation on inlet boundary layers, in controlling supersonic inlet flow unstart following downstream mass injection.

The possible use of a DBD as a means of controlling aerodynamic flows was first proposed by Roth *et al* (1998). A typical DBD actuator consists of exposed and

dielectric-covered electrodes driven by alternating current (ac). It is designed to impose a force on the ionized gas generated by the discharge and to induce a directional flow of neutral gas via collisions with the drifting ions. There have been numerous studies that have demonstrated effective subsonic flow control through separated boundary layer re-attachment (Post and Corke 2004, Huang *et al* 2006, Sung *et al* 2006, Do *et al* 2007), boundary layer transition delay (Grundmann and Tropea 2007) and turbulent boundary layer manipulation (Porter *et al* 2007, Schatzman and Thomas 2008). More recently, attention has been given to the study of the fundamental mechanisms responsible for robust actuation (Kim *et al* 2007), including the identification of strong interactions between streamwise placed actuator pairs (Do *et al* 2008). Several researchers have developed models and simulations of actuator performance (Moreau 2007). In contrast, with the exception of the work of Leonov *et al* (2005) there have been very few studies of the use of DBD actuation for the control of supersonic flows. Most studies of plasma control of supersonic flows have been limited to the use of direct current (dc) gas discharges of relatively low (Narayanaswamy *et al* 2010) and high (Leonov *et al* 2001, 2011) power. In the study reported on here, we describe the actuation of supersonic model inlet flows with relatively low power DBDs through spanwise forcing. The spanwise forcing is used to thin the turbulent boundary layer (Im *et al* 2010). We find that the control of the structure within the boundary layer has a noticeable impact on the unstart process.

In our experiments, planar laser Rayleigh scattering (PLRS) is used to visualize flow features during the unstart process, such as boundary layers, slip lines, shockwaves, and shockwave boundary layer interactions (SWBLIs). This diagnostic technique was first proposed by Miles and colleagues (Miles and Lempert 1997, Wu *et al* 2000) as a flow visualization method that is suitable in low temperature and low pressure supersonic flows. Gaseous CO_2 (added to the air stream) is condensed by the sudden temperature drop when the flow is expanded through the diverging section of a converging/diverging nozzle to form nanometer-size particles that serve to scatter the light and to provide a marker of flow structure when illuminated by a laser sheet. Shockwaves are seen as brighter features because of the higher downstream density of CO_2 particles, whereas boundary layers appear dark because of the higher temperature and concomitant CO_2 particle sublimation. This diagnostic can resolve flow features with high spatial resolution. One drawback of PLRS is that it is difficult to render the image intensity to be a quantitative indicator of flow properties. However, because of the ability to discern fine scale flow features, we use it in our studies as a means of identifying unstart shock structure.

2. Experimental setup

The experimental facility consists of a supersonic tunnel, a laser diagnostic system, and a longitudinal DBD actuator pair fabricated into the wall of a model inlet duct (integrated into the tunnel) in which air is injected through one wall, as shown schematically in figure 1. A typical in-draft blow-down wind tunnel driven by a two-dimensional converging/diverging

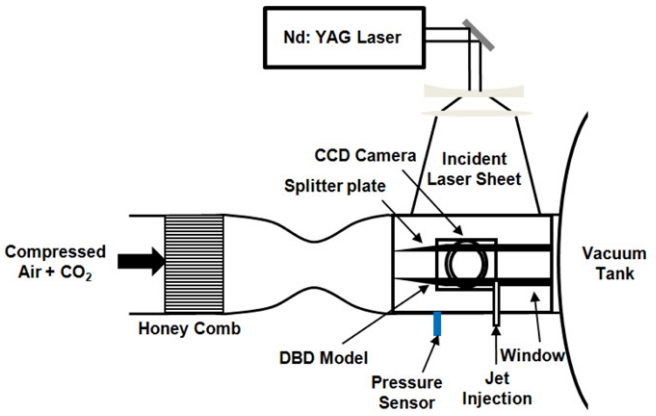

Figure 1. Schematic of the experimental setup including a supersonic wind tunnel, a pressure sensor and PLRS imaging system.

nozzle (25 : 1 area ratio) is used to produce the supersonic flow. The freestream Mach number ($Ma = 4.7 \pm 0.2$) of the base flow in the test section is determined by measuring the incident/reflected shock angle on a test wedge and is independently confirmed by PIV measurements assuming the theoretical static temperature ($T_s = 60 \pm 4$ K). A high pressure air/CO_2 mixture ($P_0 = 350$ kPa and $T_0 = 300$ K, 3 : 1 volume ratio) expands into the 40 mm × 40 mm cross sectional area tunnel test section. The useful test time is approximately 3 s. The static pressure is approximately 1 kPa. Optical access is provided by windows placed on both sides of the test section. Static pressure traces on the bottom wall of the tunnel are recorded using a fast response pressure sensor (PCB Piezotronics, Model 113B26). This pressure trace was used to determine the time to reach unstart after mass injection (discussed below).

The model inlet duct is defined by two 3 mm thick 12° wedged flat splitter plates (shown in figure 1) that span the 40 mm width of the tunnel. The upper plate is fabricated from polycarbonate to enable laser access. A DBD actuator is integrated into the upper surface of the lower plate. A portion of the plate that accommodates the DBD actuator was cast from acrylic, with an epoxy (Loctite Hysol 1C) serving as a dielectric layer (approximately 2 mm thick) isolating the buried electrode from the top exposed electrode and discharge. Both electrodes consist of a single copper metal strip, oriented parallel to the flow (streamwise direction). The exposed and buried electrodes (0.1 mm thick) are 75 mm in length and 7 mm wide, and 75 mm in length and 25 mm wide, respectively. The exposed electrode is centred over the buried electrode, and both electrodes are placed along the center of the model with the leading edge of the electrodes located 40 mm downstream from the model inlet lip. A 3 mm diameter hole is located at the end of the DBD actuator, 118 mm downstream of the leading edge, to introduce an air jet which serves as a means of injecting mass into the supersonic inlet flow. As shown in figure 2(*a*), the laser sheet (500 μm thickness) illuminates a region of interest in the flow for flow visualization. An AC power supply (GBS Elektronik GmbH, Minipuls 6) is used to drive the surface DBD discharge. A Rogowski coil (Pearson Electronics, Model 2877) and a 1000 : 1 high voltage

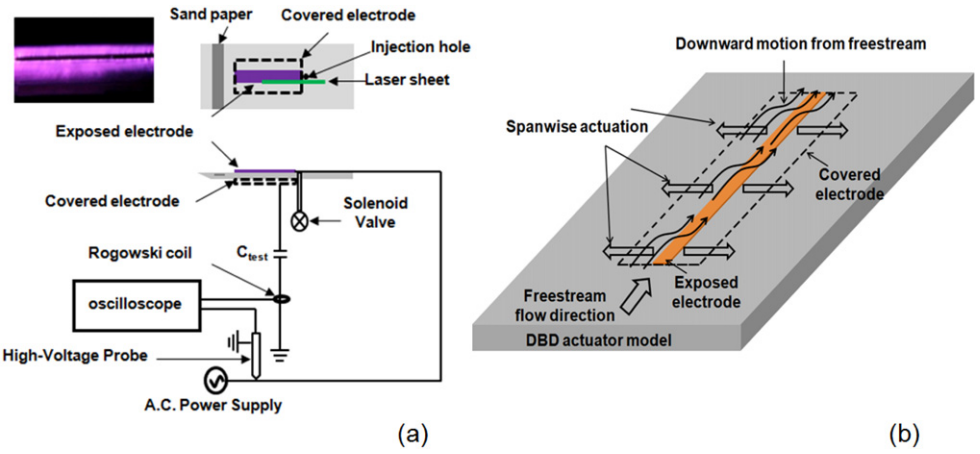

Figure 2. DBD actuator model.

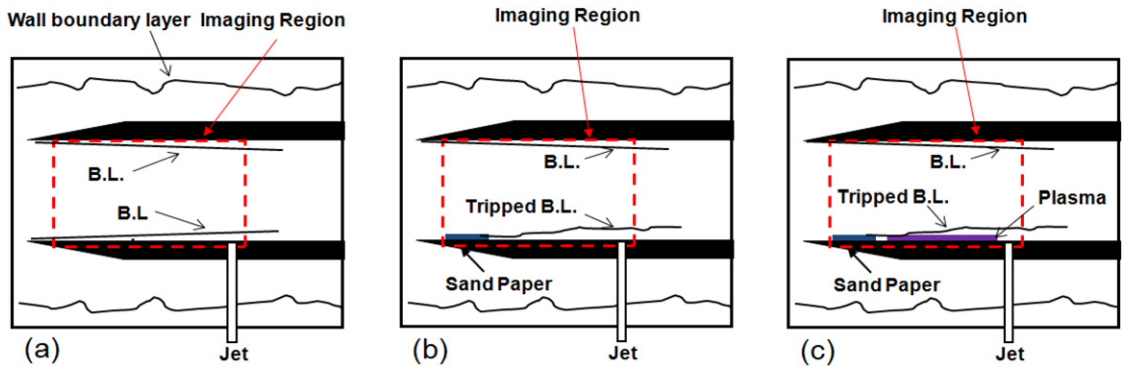

Figure 3. Schematics of flow configurations: (*a*) case I: symmetric laminar boundary layer, (*b*) case II: asymmetric tripped boundary layer, (*c*) case III: asymmetric tripped boundary layer with DBD actuation.

probe (Tektronix, P6015A) are used to record current and voltage traces, respectively. The DBD actuator is driven at 20 kHz (with the buried electrode grounded) and a 6 kV peak to peak voltage. A typical image of its emission (viewed from above) while exposed to the $Ma = 4.7$ flow taken by a digital camera with 1/30 s exposure time is presented as the inset to figure 2(*a*). Figure 2(*b*) illustrates schematically, the spanwise forcing generated by the actuator and the effect that this forcing is believed to play on boundary layer thinning. A DBD actuator pair (exposed and covered electrodes) produces a spanwise directional flow relative to the freestream flow and this motion draws higher momentum fluid down towards the surface.

A Nd : YAG laser (New wave, Gemini PIV, 100 mJ/pulse energy, 10 Hz, 532 nm) is shaped into a thin sheet using two cylindrical lenses ($f = 200$ mm) and a convex spherical lens ($f = 250$ mm), and directed into the test section for the PLRS diagnostic. A CCD camera (La Vision, Imager Intense, 1376 × 1040 pixel array) detects the scattered light at 90° to the plane of the laser sheet. Laser firing for the PLRS is synchronized to the CCD camera exposure (3 μs). Phase-locking is used to investigate phase dependency on the DBD actuation. Laser firing is triggered by the rise in discharge voltage as obtained using a high voltage probe on the powered lead, and is delayed to acquire images at different phases using a pulse delay generator (SRS, DG 535). It is found that the robustness of the DBD actuator has a dependence on the phase within the AC cycle. The images shown in figure 6 are for phase delays (90°, see figure 7) at which the actuation is seen to be the strongest. In all of the experiments, an output reference from the laser Q-switch is used to trigger the jet injection and is delayed as desired by a pulse delay generator (SRS, DG 535). The mass injection is controlled by a solenoid valve (ASCO, Red Hat II) driven by a controller (Optimal Engineering System Inc.), receiving its trigger from the delay generator. For the studies reported here, a sonic jet (air, 100 psi stagnation pressure and ambient stagnation temperature) is injected into the test section through the 3 mm diameter hole in the DBD model resulting in a flow disturbance/blockage and an overall increase in flow pressure and temperature.

Three flow configurations are considered for these studies, as depicted in figure 3. In all cases, two wedged plates are used to define the model inlet flow. With these plates, the inlet flow is fully isolated from the lower and upper wall turbulent boundary layers, but it is still exposed to the thick (~1 cm) turbulent boundary layers on the side walls. The height of the model flow is 15 mm. In the first configuration (case I), boundary layers grow naturally from the leading edge of each plate. For cases II and III, sand paper (120 Grit, 40 mm wide and 20 mm long) is attached to the bottom plate starting 10 mm downstream from the leading edge (to just upstream of the DBD) to trip the otherwise laminar boundary layer, creating

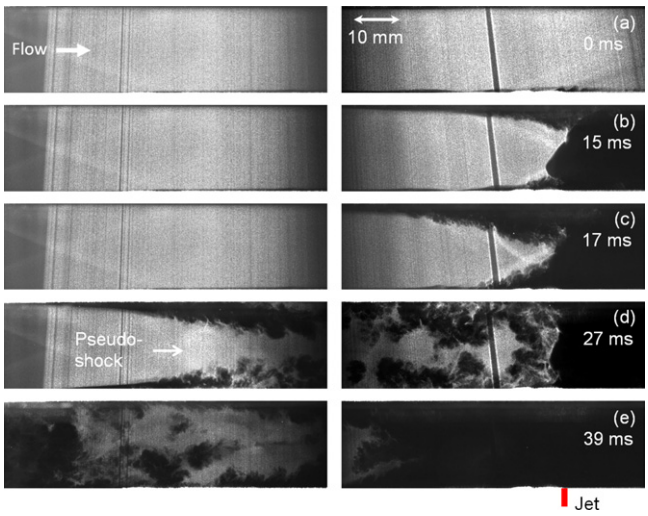

Figure 4. Time sequential PLRS images of unstart with the case I flow configuration.

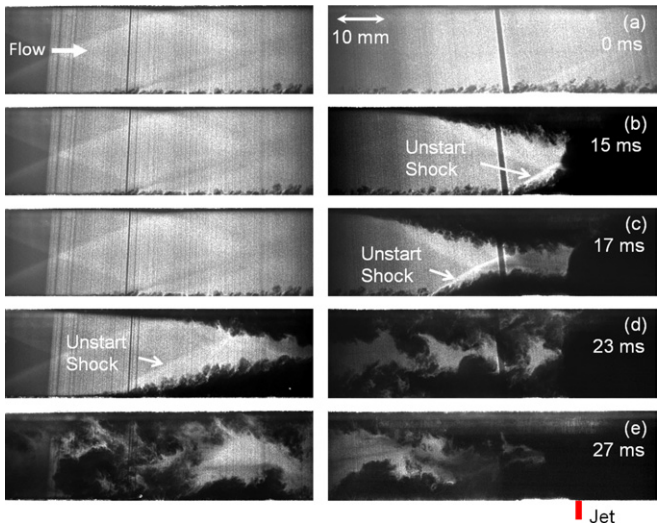

Figure 5. Time sequential PLRS images of unstart with the case II flow configuration.

a relatively thick boundary layer. The DBD actuator is only activated in the case III flow configuration.

3. Results

3.1. Unstart dynamics

The time-evolving flow features that are induced following mass injection for cases I–III are depicted in figures 4–6, respectively. The time stamp in the right frame of the image represents the time following the triggering of the jet. Two frames from separate interrogation regions are concatenated to span an overall distance of 130 mm along the inlet flow. The right frames illuminate the region in the vicinity of the injected jet whereas the left frames depict the upstream region of the flow closer to inlet lip. The darker vertical band in the right frames is an image artefact. All images are taken with the laser sheet aligned with the edge of the exposed electrode. The thickness of the boundary layers can be estimated (qualitatively) by measuring the height of the dark region on the plates (Poggie *et al* 2004). For quantitative comparison, velocity profiles are measured for three cases at 108 mm downstream of the model inlet with a pitot probe.

Figure 4(*a*) depicts undisturbed flow of case I prior to mass injection, with initially symmetric thin laminar boundary layers. Figure 4(*b*) visualizes the flow shortly after mass injection, showing that separated boundary layers and oblique shockwaves form close to the jet injection location resulting in a strong disruption in the flow field. These boundary layers thicken, with separation points appearing to move upstream in time. At 17 ms, we see the appearance of symmetric oblique shockwaves just upstream of the point of injection. By 27 ms (see figure 4(*d*)) these shockwaves merge to form a quasi-stationary pseudo-shock (Arai *et al* 1990), or region in which compression waves coalesce, approximately 70 mm upstream of the point of mass injection. Eventually (by 37 ms, for these conditions), this pseudo-shock structure breaks down as the pressure increases behind it, followed nearly immediately by inlet unstart (figure 4(*e*)).

A similar time dependent behaviour is depicted in figure 5 for the unstart process associated with the case II flow configuration. However, the initial undisturbed flow has a relatively thick boundary layer on the lower wall due to the boundary layer tripping (see figure 5(*a*)). As a result of this asymmetric boundary layer condition case II evolves to form one single oblique shock just upstream of the separated flow in the lower boundary layer (figures 5(*b*) and (*c*)). This oblique shock propagates upstream along with the thickened region of the boundary layer, and unlike case I, does not coalesce into a pseudo-shock, nor does it appear to become quasi-stationary. Instead, it continuously moves upstream at a near constant speed until it reaches the model lip, after which it is followed by a nearly complete unstart of the inlet (figure 5(*e*)). The overall time to unstart following mass injection is shorter by ∼10 ms for the case II configuration when compared with case I. Interestingly, this time is about the time for which the pseudo-shock remains stationary in the case I configuration. It is apparent that unstart of inlet flows are strongly affected by boundary layer characteristics (e.g. symmetric or asymmetric). It is this finding, which is also described in similar experiments by Do *et al* (2011a, 2011b), which prompted our conjecture that unstart can be delayed by appropriate actuation of inlet flow boundary layers.

The use of DBD actuation of the flow to manipulate this unstart process is tested for the case II configuration with an activated discharge (case III). Flow visualizations at various times following jet triggering are shown in figure 6. It is apparent that the thickness of the boundary layer under initial steady-state conditions (prior to mass injection) on the lower wall is significantly reduced with the DBD activated (see figure 6(*a*)). This apparent thinning of the boundary layer is consistent with our earlier reports (Im *et al* 2010). We see however, that the discharge starts to lose its effectiveness in the downstream portion of the actuator where there is a resurgence of the boundary layer growth. Again, there is the appearance of an oblique unstart shockwave on the DBD actuator side (figures 6(*b*) and (*c*)) following mass injection. Recall that in

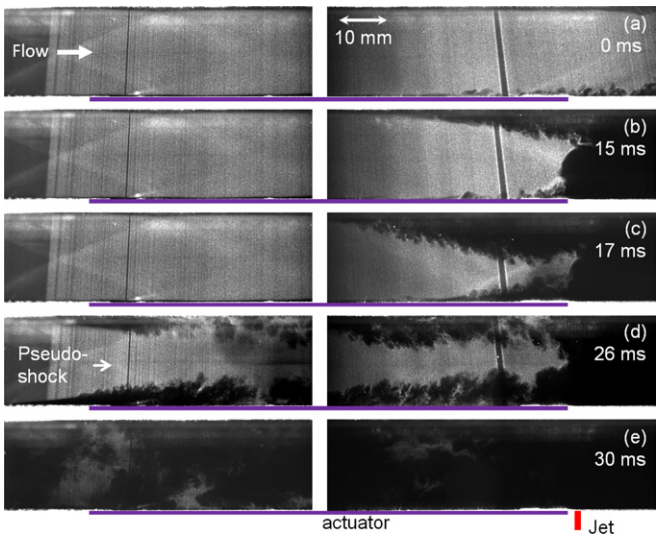

Figure 6. Time sequential PLRS images of unstart with the case III flow configuration.

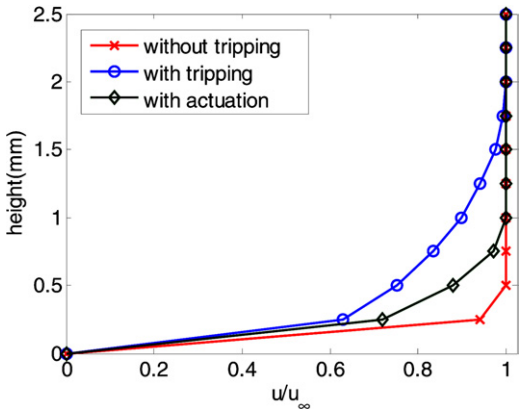

Figure 7. Freestream velocity profile along the height of the model inlet flow for case I (without tripping), case II (with tripping), case III (with actuation).

case II, this oblique shockwave, forming on the initially thicker boundary layer side, propagates upstream as an oblique shock at near constant speed. Interestingly, we find that when the unstart shock reaches the region that is effectively actuated by the DBD, it takes on the characteristics of the pseudo-shock seen in case I studies. This pseudo-shock appears to be quasi-stationary (for approximately 2–3 ms) at a location of 70 mm upstream of the mass injection location (see figure 6(*d*)). Although the lifetime of this pseudo-shock is shorter than that observed for case I, it is nevertheless apparent that the unstart dynamics is affected by DBD actuation, and results in the transition from an initially oblique shock propagation to a quasi-stationary pseudo-shock. As seen for case I, the eventual increase in pressure behind this pseudo-shock results unstart, as shown in figure 6(*e*).

The freestream velocity profiles for cases I–III are determined by pitot probe measurements taken on the inlet lower plate centreline 10 mm upstream of the jet. The 500 μm outer and 250 μm inner diameter pitot probe accessed the model inlet flow through the jet injection hole. The measured velocity profiles are plotted in figure 7. The boundary

Table 1. Boundary layer thickness (δ), displacement thickness (δ^*), momentum thickness (θ), and shape factor (H) for cases I–III.

Flow condition	δ (mm)	δ^* (mm)	θ (mm)	H
Case I	0.5	0.28	0.013	21.54
Case II	2.0	0.66	0.150	4.40
Case III	1.0	0.43	0.069	6.23

layer thickness (δ), displacement thickness (δ^*), momentum thickness (θ), and shape factor (H) for each flow condition is given in table 1. The boundary layer thickness without flow tripping (case I) estimated from the velocity profile is $\delta = 0.5$ mm. This is consistent with theoretical estimates (Schlichting 1955) for $Re_x = 1.5 \times 10^6$. On the other hand, the tripped case 2 results in a boundary layer that is thickened (as expected) to $\delta = 2$ mm at this same location. The case II condition, when actuated (case III), is seen to thin the boundary layer to approximately 1 mm as shown in figure 7 and indicated in table 1. It is apparent that while the plasma actuation clearly reduces the boundary layer thickness it could not completely thin the boundary layer down to that measured for the untripped case (case I). Nevertheless, the effect of actuation on the boundary layer is robust and is consistent with the flow behaviour seen in figures 4–6.

3.2. Time to unstart

A quantitative measure in how effective the plasma actuator is in delaying unstart is the statistical significance in the time interval between the jet injection trigger signal and the eventual rise in pressure at the inlet lip, as measured with and without tripping and plasma actuation. This time interval can be determined by monitoring the pressure on the lower wind tunnel wall just downstream of the model. Figures 8(*a*) and (*b*) depict schematically the qualitative flow conditions outside of the model inlet before and after unstart, respectively. Before unstart, the flow surrounding the model inlet is relatively undisturbed and the pressure sensor signal, shown in figure 8(*c*), is steady and stable. However, once the shock propagates upstream of the model inlet—i.e. after model unstart, the surrounding flow is strongly disturbed (figure 8(*b*)) and there is a rapid pressure rise on the tunnel wall some time interval, Δt, following the jet injection trigger (figure 8(*c*)).

Probability distribution functions describing this unstart time interval are presented in figure 9. These distributions are generated by carrying out more than one hundred experiments for each flow configuration (cases I–III). Both histograms and superimposed best-fit normal (Gaussian) distributions are shown for each case, with the dotted line (blue), solid line (green), and dashed line (red) representing the results for Case I, II, and III respectively. The peaks of these distributions appear at time intervals of 39.2 ms, 27.6 ms and 30.3 ms for cases I, II, and III, respectively. There is a relatively large interval of 11.6 ms between cases I and II due to the quasi-stability of the pseudo-shock seen in case I, but absence in case II. We see that the unstart time is delayed by approximately 2.7 ms by applying DBD actuation. This delay is attributed to the downward flow induced by the spanwise flow generated by

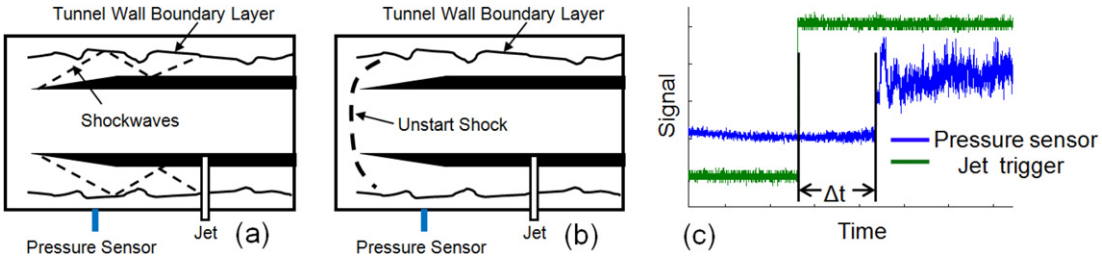

Figure 8. Schematic of flow conditions: (*a*) before unstart, (*b*) after unstart and (*c*) definition of time to unstart, Δt.

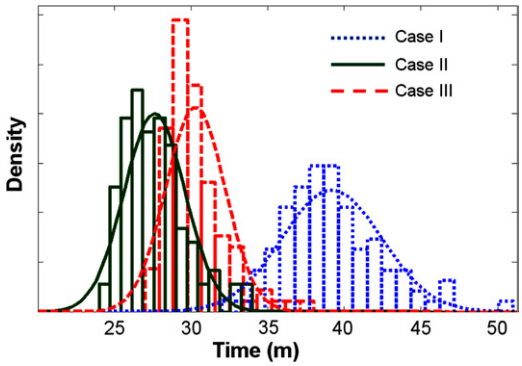

Figure 9. Time to unstart, Δt, histogram for each flow configuration. The lines represent a best fit to a normal (Gaussian) distribution.

the actuator, bringing higher velocity fluid into the boundary layer, as shown schematically in figure 2(*b*). While statistically significant, this delay is only 23% of that seen between cases I and II.

3.3. Limiting factors

Improvements in the actuator performance and robustness in delaying inlet unstart will require detailed studies of how the actuator functions. As mentioned above, it is believed that actuation is the result of the induced downward flow which carries streamwise momentum into the boundary layer. This downward flow is expected to be strongest near the edge of the exposed electrode where the electric field is believed to be strongest. It is expected then, that boundary layer thinning will be strongly dependent on the spanwise coordinate.

The spanwise variation in boundary layer characteristics are visualized by recording PLRS images with the illuminating laser sheet location traversed away from the edge of the exposed electrode. Rayleigh scattering images of the flow with the sheet coincident with a plane passing through the exposed electrode edge, 1.5 mm from the edge, and 3 mm from the edge are depicted in figures 10(*a*), (*b*), and (*c*), respectively with DBD actuation (case III). Relatively strong boundary layer thinning is seen at the electrode edge (figure 10(*a*)). However, this plasma-enhanced boundary layer thinning diminishes rapidly with spanwise displacement, as seen in figures 10(*b*) and (*c*). Beyond 3 mm from the exposed electrode edge, the thickness and qualitative structure of this boundary layer is similar to that of the tripped boundary layer without DBD actuation. We find that boundary layer thinning is confined

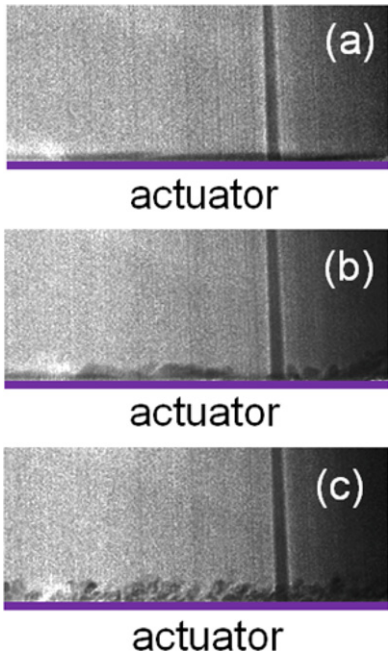

Figure 10. PLRS images of (*a*) exposed electrode edge, (*b*) 1.5 mm from the edge and (*c*) 3 mm from the edge.

to a relatively small region of the flow within the immediate vicinity of the actuator edge. Future experiments are needed to understand how modifications to the actuator design or operation can broaden this spanwise actuation range.

It is also well known from studies in subsonic flow actuation that this ac DBD generates a force on the flow that is strongly phase dependent (Do *et al* 2008, Little *et al* 2009). To understand the phase dependence of this downward flow under supersonic flow conditions, we have captured phase-resolved visualizations of the flow in the vicinity of the exposed electrode edge. The timing of the images taken at five phase shifts (0, $\pi/4$, $\pi/2$, π, and $3\pi/2$) within a single ac voltage cycle is depicted in figure 11, denoted as (*a*), (*b*), (*c*), (*d*) and (*e*), respectively. Also shown in figure 11 is the discharge current. The corresponding PLRS images for each phase are illustrated in figures 11(*a*), (*b*), (*c*), (*d*), and (*e*) respectively. The visualizations in figure 12 correspond to an imaging window spanning 85 to 110 mm from the model leading edge and a 10 mm height. It is seems that there is little or no actuation at zero phase (figure 12(*a*)). Slight evidence of actuation is seen in figure 12(*b*). The strongest actuation is seen at a phase shift of 90°, as apparent in the image of figure 12(*c*). Boundary layer actuation diminishes strongly at greater phase shifts

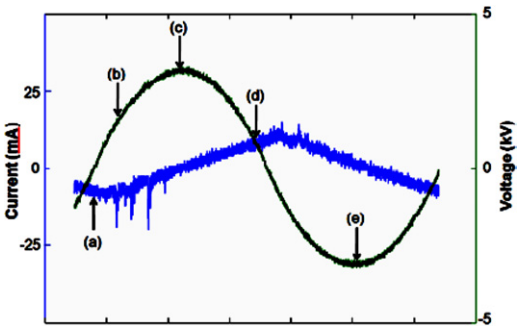

Figure 11. Typical voltage and current traces for the DBD actuator.

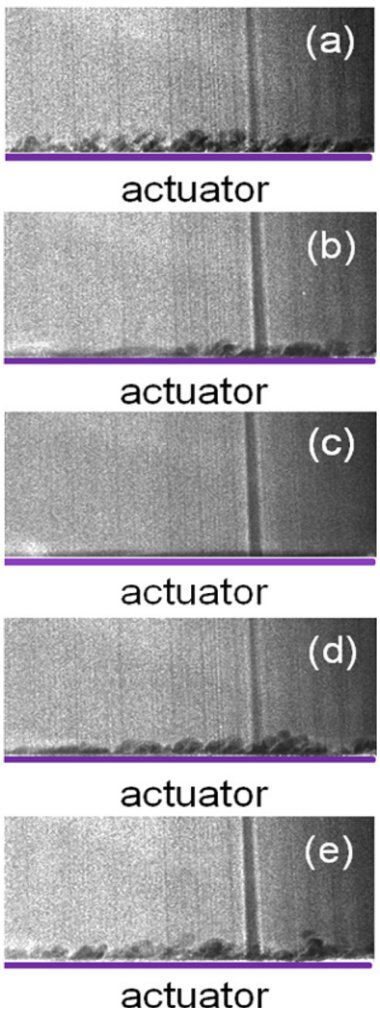

Figure 12. Phase-locked PLRS images at the exposed electrode edge: (*a*) 0°, (*b*) 45°, (*c*) 90°, (*d*) 180° and (*e*) 270°.

(figures 12(*d*) and (*e*)). These findings (both the spanwise and phase dependence on actuation) suggest that perhaps adjacent asymmetric actuators shifted appropriately in phase from the central symmetric actuator may be one method of enhancing actuator performance.

4. Summary

A DBD actuator is studied as a possible means of manipulating unstart processes in a model supersonic inlet flow. This experiment generates unstart in a $Ma = 4.7$ model inlet by downstream sonic jet mass injection. PLRS from condensed CO_2 particles is used as a flow visualization method to mark flow features such as boundary layer thickness, separation, and shockwaves. Three inlet model flow configurations are considered with varying initial boundary layer conditions. For the first configuration (case I), the upper and lower wall of the model have initially laminar boundary layers that grow naturally from each plate's leading edge. As a result of this symmetric and thin boundary layer flow, a pseudo-shock appears during the unstart of the inlet and this pseudo-shock is found to be quasi-stationary for a period of about 10 ms. This pseudo-shock eventually breaks down as a result of the continuously rising pressure rise behind it. In the second configuration (case II), a relatively thick tripped boundary layer is intentionally generated on the lower plate. With this asymmetric boundary layer flow condition there is no pseudo-shock, and instead, a relatively strong oblique unstart shock appears, rooted on the lower, thicker boundary layer side. This shock precedes the separating boundary layer and propagates upstream at nearly constant speed until it reaches the inlet entrance. Unstart occurs shortly after this oblique shock leaves the inlet. The third case (case III), is just the case II condition, but with DBD actuation applied to partially arrest the propagation of this separating boundary layer disturbance. PLRS visualization suggests that local boundary layer thinning occurs with DBD actuation with the oblique unstart shock transitioning to a structure that resembles the pseudo-shock seen with the symmetric boundary layer flow (case I). This pseudo-shock is also quasi-stationary but is quasi-stable for a time considerably shorter than that seen in case I (by approximately 30%). A closer examination of the DBD actuation by PLRS imaging regions across the exposed electrode indicates that the boundary layer thinning is limited in area to regions in close proximity to the electrode. Phase-resolved PLRS visualization also indicates that the strongest actuation occurs at a phase shift of 90° in the sinusoidal voltage cycle.

Acknowledgments

This work is conducted through support provided by the Stanford Predictive Science Academic Alliance Program (PSAAP) Center, funded by the Department of Energy (National Nuclear Security Administration) under Award Number DE-FC52-08NA28614. Authors thank to Dr M Godfrey Mungal for providing the laser system and helpful discussions and Mr Benjamin Wang for helping with some measurements.

References

Arai T, Sugiyama H, Abe F, Takahashi T and Onodera O 1990 Internal structure of pseudo-shock waves in a square duct *AIP Conf. Proc.* **208** 850–5

Curran E T, Heiser W H and Pratt D T 1996 Fluid phenomena in scramjet combustion systems *Annu. Rev. Fluid Mech.* **28** 323–60

Do H, Kim W, Mungal M G and Cappelli M A 2007 Bluff body flow separation control using surface dielectric barrier discharges

45th AIAA Aerospace Sciences Meeting and Exhibit (Reno, NV) paper 2007-939

Do H, Kim W, Cappelli M A and Mungal M G 2008 Cross-talk in multiple dielectric barrier discharge actuators *Appl. Phys. Lett.* **92** 071504

Do H, Im S, Mungal M G and Cappelli M A 2011a Visualizing supersonic inlet duct unstart using planar laser Rayleigh scattering *Exp. Fluids* **50** 1651–7

Do H, Im S, Mungal M G and Cappelli M A 2011b The influence of boundary layer on supersonic inlet flow unstart induced by mass injection *Exp. Fluids* **51** 679–91

Emami S, Trexler C A, Auslender A H and Weidner J P 1995 Experimental investigation of inlet-combustor isolators for a dual-mode scramjet at a Mach number of 4 *NASA Technical Paper* 3502

Grundmann S and Tropea C 2007 Experimental transition delay using glow-discharge plasma actuators *Exp. Fluids* **42** 653–7

Heiser W H and Pratt D T 1994 *Hypersonic Air Breathing Propulsion* AIAA Education Series (Reston, VA: AIAA)

Huang J, Corke T C and Thomas F O 2006 Unsteady plasma actuators for separation control of low-pressure turbine *AIAA J.* **44** 1477–87

Im S, Do H and Cappelli M A 2010 Dielectric barrier discharge control of a turbulent boundary layer in a supersonic flow *Appl. Phys. Lett.* **97** 041503

Kim W, Do H, Mungal M G and Cappelli M A 2007 On the role of Oxygen in dielectric barrier discharge actuation of aerodynamic flows *Appl. Phys. Lett.* **91** 181501

Kodera M, Tomioka S, Kanda T, Mitani T and Kobayashi K 2003 Mach 6 test of a scramjet engine with boundary-layer bleeding *12th AIAA Int. Space Planes and Hypersonic Systems and Technologies (Norfolk, VA)* paper 2003-7049

Leonov S B, Bityurin V, Savischenko N, Yurev A and Gromov V 2001 Influence of surface electrical discharge on friction of plate in subsonic and transonic airflow *39th AIAA Aerospace Sciences Meeting and Exhibit (Reno, NV)* paper 2001-640

Leonov S B, Bityurin V A, Yarantsev D A, Isaenkov Y I and Soloviev V R 2005 High-speed flow control due to interaction with electrical discharges *13th AIAA International Space Planes and Hypersonic Systems and Technologies Conf. (Capua, Italy)* paper 2005-3287

Leonov S B, Firsov A A, Yarantsev D A, Falempin F and Goldfeld M A 2011 Plasma effect on shocks configuration in compression ramp *17th AIAA Int. Space Planes and Hypersonic Systems and Technologies Conf. (San Francisco, CA)* paper 2011-2362

Little J, Nishihara M, Adamovich I and Samimy M 2009 Separation control from the flap of a high-lift airfoil using DBD plasma actuators *47th AIAA Aerospace Sciences Meeting including the New Horizons Forum and Aerospace Exposition (Orlando, CA)* paper 2009-145

Mashio S, Kurashina K, Bamba T, Okimoto S and Kaji S 2001 Unstart phenomenon due to thermal choke in scramjet module *AIAA/NAL-NASDA-ISAS 10th Int. Space Planes and Hypersonic Systems and Technologies Conf. (Kyoto)* paper 2001-1887

McDaniel K S and Edwards J R 2001 Three-dimensional simulation of thermal choking in a model scramjet combustor *39th Aerospace Sciences Meeting and Exhibit (Reno, NV)* paper 2001-382

Miles R B and Lempert W R 1997 Quantitative flow visualization in unseeded flows *Annu. Rev. Fluid. Mech.* **29** 285–326

Moreau E 2007 Airflow control by non-thermal plasma actuators *J. Phys. D: Appl. Phys.* **40** 605–36

Narayanaswamy V, Raja L L and Clemens N T 2010 Characterization of a high-frequency pulsed-plasma jet actuator for supersonic flow control *AIAA J.* **48** 297–305

O'Byrne S, Doolan M, Olsen S R and Houwing A F P 2000 Analysis of transient thermal choking processes in a model scramjet engine *J. Propulsion Power* **16** 808–14

Poggie J, Erbland P J, Smits A J and Miles R B 2004 Quantitative visualization of compressible turbulent shear flows using condensate-enhanced Rayleigh scattering *Exp. Fluids* **37** 438–54

Porter C O, Baughn J W, McLaughlin T E, Enloe C L and Font G I 2007 Plasma actuator force measurements *AIAA J.* **45** 1562–70

Post M L and Corke T C 2004 Separation control on high angle of attack airfoil using plasma actuators *AIAA J.* **42** 2177–84

Rodi P E, Emami S and Trexler C A 1996 Unsteady pressure behavior in a ramjet/scramjet inlet *J. Propulsion Power* **12** 486–93

Roth J R, Sherman, D M and Wilkinson S P 1998 Boundary layer flow control with a one atmosphere uniform glow discharge surface plasma *36th AIAA Sciences Meeting and Exhibit (Reno, NV)* paper 1998-328

Sato S, Izumikawa M, Tomioka S and Mitani T 1997 Scramjet engine test at Mach 6 flight Condition *33rd AIAA/ASME/SAE/ASEE Joint Propulsion Conf. and Exhibit (Seattle, WA)* paper 1997-3021

Schatzman D M and Thomas F O 2008 Turbulent boundary layer separation control using plasma actuators *4th AIAA Flow Control Conf. (Seattle, WA)* paper 2008-4199

Schlichting H 1955 *Boundary Layer Theory* (New York: McGraw-Hill)

Sung Y, Kim W, Mungal M G and Cappelli M A 2006 Aerodynamic modification of flow over bluff objects by plasma actuation *Exp. Fluids* **41** 479–86

Tam C, Eklund D and Behdadnia R 2008 Influence of downstream boundary conditions on scramjet-isolator simulations *26th AIAA Applied Aerodynamics Conf. (Honolulu, HI)* paper 2008-6929

Wagner J L, Yuceil K B, Valdivia A, Clemens N T and Dolling D S 2008 PIV measurements of the unstart process in a supersonic inlet/isolator *38th Fluid Dynamics Conf. and Exhibit (Seattle, WA)* paper 2008-3849

Wang X and Le J 2000 Computations of inlet/isolator for SCRAMjet engine *J. Therm. Sci.* **9** 334–8

Wieting A R 1976 Exploratory study of transient unstart phenomena in a three-dimensional fixed-geometry scramjet engine *NASA Technical Note* TN D-8156

Wu P, Lempert W R and Miles RB 2000 Megahertz pulse-burst laser and visualization of shock-wave/boundary-layer interaction *AIAA J.* **38** 672–9